Thermochimica Acta 494 (2009) 45–53

Contents lists available at ScienceDirect

Thermochimica Acta

journal homepage: www.elsevier.com/locate/tca

Thermolysis of new hybrid silsesquioxane–carbosilane materials

Anna Kowalewska[a,*], Witold Fortuniak[a], Krystyna Rózga-Wijas[a], Bartosz Handke[b]

[a] Centre of Molecular and Macromolecular Studies, Polish Academy of Sciences, Sienkiewicza 112, 90-363 Łódź, Poland
[b] AGH University of Science and Technology, Faculty of Materials Science and Ceramics, Al. Mickiewicza 30, 30-059 Kraków, Poland

ARTICLE INFO

Article history:
Received 15 January 2009
Received in revised form 17 April 2009
Accepted 21 April 2009
Available online 3 May 2009

Keywords:
Thermolysis
Silsesquioxane
Carbosilane
Tris(trimethylsilyl)methane

ABSTRACT

Thermal decomposition of new silsesquioxane materials $[(Me_3Si)_3CSiMe_2CH_2CH_2SiO_{3/2}]_n$ ($PT_{Si}SS$), substituted with sterically hindered carbosilane groups, was studied in an inert atmosphere (N_2) and air. It was found that a specific degradation of carbosilane moieties occurs at high temperatures. A ceramic residue was obtained > 900 K both in nitrogen ($Si_xO_yC_z$) and air (Si_xO_y). Thermal rearrangements in the structure of polyhedral and ladder-like $PT_{Si}SS$ were studied, and related to those observed for a polymethylsilsesquioxane resin (PMSS) of regular ladder-like architecture. Thermally induced transformations were evaluated by TGA(DTA)-MS, FTIR, NMR, XRD and SEM.

1. Introduction

Polyhedral silsesquioxane units introduced into polymeric nanocomposite materials can improve their thermal, mechanical and dielectric properties [1–10]. The investigation of their decomposition at high temperatures can provide an insight into the system stability and explain the mechanism of conversion into a ceramic material [11]. Thermolysis of various octahedral [12–17] and polymeric [18–30] silsesquioxanes has been thus studied. Completely condensed octahedral POSS {T_8^R, R=*c*-C_6H_{11} [12], C_nH_{2n+1} (n = 2–10) [13], Me, Vi, *i*-Bu, *i*-Oct [14], $CH_2CH_2OCH_2CH_2Cl$ [15], $OSiMe_2H$ [16], $OSiMe_2CH_2CH_2Ph$ [17]} were found to sublime on heating in an inert atmosphere. It was shown that on increasing the length of alkyl chain from C_2 to C_{10} in octahedral POSS the weight loss onset (due to volatilisation and decomposition) shifted to higher temperatures [13]. Octahedral POSS with simple organic substituents that do not sublime at elevated temperatures in N_2 can be found among these tending to form chars of aromatic structure on decomposition. T_8Ph is thermally stable up to 620 K in N_2 and leaves 70% of ceramic residue > 1000 K [14]. Acetoxyphenyl and hydroxyphenyl substituted POSS, capable of hydrogen bonding, gave respectively 60% and 70% char yields at 1100 K [17]. Very recently we have reported preparation of a new type of hybrid silsesquioxane materials – $[(Me_3Si)_3CSiMe_2CH_2CH_2SiO_{3/2}]_n$ ($PT_{Si}SS$) – bearing a sterically hindered tris(trimethylsilyl)methyl (T_{Si})-type ligands [31] .They are built of octahedral or ladder-like silsesquioxane framework surrounded by nonpolar carbosilane ligands. Contrary to common octahedral T_8 molecules, $[(Me_3Si)_3CSiMe_2CH_2CH_2SiO_{3/2}]_8$ ($PT_{Si}SS$-I, Scheme 1) do not sublime on heating in nitrogen atmosphere. Comparative thermogravimetric analysis [32] of octahedral silsesquioxanes functionalized with typical organic groups (Me, Vi, Ph) and $PT_{Si}SS$-I points out to the unique properties of the latter. Bulky T_{Si} groups were already shown to provide an exceptional steric protection to polymeric systems, resulting in an effective separation of polymeric chains and a substantial decrease in their mobility [33–38]. Consequently, an improved material performance, glass transition temperature increase and thermal resistance enhancement are observed. Octahedral, crystalline ($PT_{Si}SS$-I) and ladder-like, polymeric ($PT_{Si}SS$-II) silsesquioxanes bearing T_{Si} groups were thus examined for the structural changes occurring during their thermolysis.

It is known that the steric strain within T_{Si} ligand is decreased by a specific arrangement of Me_3Si-substituents about the central carbon atom [39–41]. Due to the significant difference in the length of Si—C bonds within T_{Si} moiety (inner Si—C_q and outer Si—CH_3), breaking of the former was found to be more feasible during UV-laser induced decomposition of siloxanes with side tris(trimethylsilyl)hexyl groups [35]. The difference in the bond length between inner Si—C_q and outer Si—CH_3 in T_{Si} moiety is also the cause of a particular thermal transition and heat capacity change in $PT_{Si}SS$. Combined DSC and variable temperature NMR (^{29}Si and ^{13}C) methods indicated an increase in mobility of Me_3Si groups above this temperature [31]. The finding was thought to be of importance for the mechanism of thermolysis of $PT_{Si}SS$. Accordingly, it was expected that C—$SiMe_3$ bonds would break easily at

* Corresponding author. Tel.: +48 4268 03203; fax: +48 4268 47126.
E-mail address: anko@cbmm.lodz.pl (A. Kowalewska).

0040-6031/$ – see front matter © 2009 Elsevier B.V. All rights reserved.
doi:10.1016/j.tca.2009.04.016

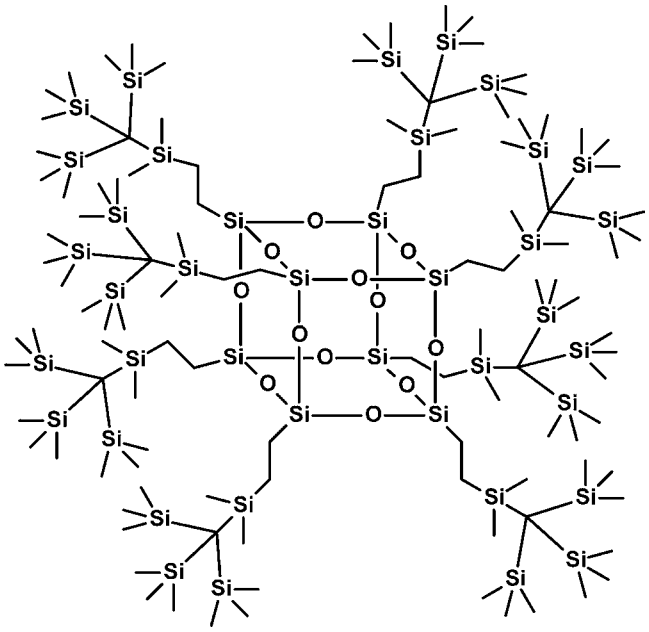

Scheme 1. Structure of $PT_{Si}SS$-I.

high temperatures. Such an easy decomposition of the carbosilane moiety (with formation of volatile products) in a POSS-type material could give a possibility for high temperature studies of Si—O—Si bonds rearrangement in a completely inorganic system of a well-organized structure. The study of the thermal decomposition of two available types of $PT_{Si}SS$ [octahedral $PT_{Si}SS$-I and polymeric, ladder-like $PT_{Si}SS$-II (Scheme 2)] in comparison to a ladder-like polymethylsilsesquioxane [PMSS (Scheme 3)] was thus undertaken. The chars were analyzed by NMR, XRD, FTIR and SEM. The volatile products of thermolyses were identified by TG(DTA)-MS studies.

2. Experimental section

2.1. Characteristics of the used silsesquioxane materials

$PT_{Si}SS$ were obtained as previously reported [31]. $PT_{Si}SS$-I is composed of regular, crystalline octahedral species (characteristic XRD lines at 2θ=5.96° and 2θ=11.86°). Polymeric $PT_{Si}SS$-II shows two characteristic broad lines in its XRD spectra, corresponding to spacing of 17.3 Å ($2\theta = 5.1^\circ$) and 7.5 Å ($2\theta = 11.8^\circ$). Degree of hydrolysis of alkoxysilyl groups in $PT_{Si}SS$-II by ^{1}H NMR = 98.4%, molecular weight Mn_{RI} = 1500 D, PDI_{RI} = 1.1, Mn_{MALLS} = 3900 D, PDI_{MALLS} = 1.0. A lamellar order with spatial arrangement of 4.1 nm was found in PTSiSS-II (SAXS).

PMSS was obtained by hydrolytic condensation of 2,4,6,8-tetraethoxy-2,4,6,8-tetramethylcyclotetrasiloxane, carried out in EtOH and catalyzed by tetrabutylammonium fluoride [42,43]. The

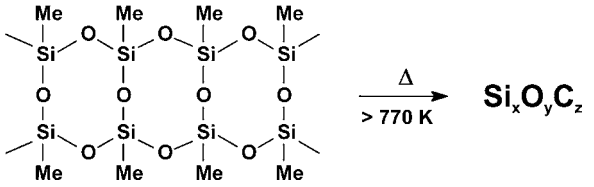

Scheme 3. Ceramization of a polmethylysilsesquioxane (PMSS) containing 4-fold siloxane rings in its structure.

used method allows for preparation of PMSS of regular ladder-like structure. Prior to the thermal analysis, PMSS was purified from traces of octahedral methylsilsesquioxane $(CH_3SiO_{3/2})_8$ which were removed by its careful volatilisation at 370 K under high vacuum.

2.2. Analysis and general methodology

Solid state MAS NMR spectra were recorded on a Bruker MSL-300 MHz spectrometer (59.6 MHz for ^{29}Si and 75.5 MHz for ^{13}C) using a Bruker CP MAS probe with a 4 mm zirconium rotor. The peak positions were referenced to the signal of Q_8M_8 (trimethylsilyl ester of cubic octameric silicate) standard.

The structure was detected by wide-angle X-Ray powder diffraction measurement (WAXS) performed using Philips X'Pert Pro MD diffractometer. Radiation used was Cu Kα1 line monochomatized by Ge(1 1 1) monochromator. Standard Bragg–Brentano geometry with Θ–2Θ setup was applied (0.008° step size and 5–90° 2Θ range). Small-angle X-ray scattering (2D SAXS) measurement was carried out using a 1.1-m-long Kiessig-type camera, equipped with a pinhole collimator and coupled to an X-ray generator (sealed-tube, fine-point Cu Kα-filtered source operating at 50 kV and 35 mA).

FTIR spectra were recorded with FT-IR ATI Mattson Spectrometer. Samples were prepared with the standard potassium bromide pellet technique.

Thermogravimetric analyses were performed by the use of a TGA 2950 Thermogravimetric Analyzer (TA Instruments) in nitrogen or air atmosphere (heating rate 10 K/min). Thermolysis, in the flow of N_2 or air, of all studied samples was carried out under TGA set conditions (heating rate 10 or 20 K/min, as specified in the text) using TGA 2950 with a platinum heating pan.

The analysis of gaseous products of decomposition was carried out using a quadrupole mass spectrometer (QMD 300 Thermostar Balzers) connected on-line with SDT 2960 apparatus (TA Instruments) by a heated quartz capillary. Samples were heated to 1270 K (10 K/min) in a standard platinum sample pan. The experiments were carried out in dynamic flow of helium [99.999%, however the spectrometer detected a certain amount of H_2O (m/z = 18 and 17) as well as O_2 (m/z = 32 and 16)] or in synthetic air (<15 ppm H_2O). The gas flow rate was 5 dm^3/h and the volume of thermoanalyzer was 0.06 dm^3. The mass spectrometer was operated with an electron impact ionizer with energy 0.112 aJ (70 eV). Mass spectra were recorded for m/z range 10–99.

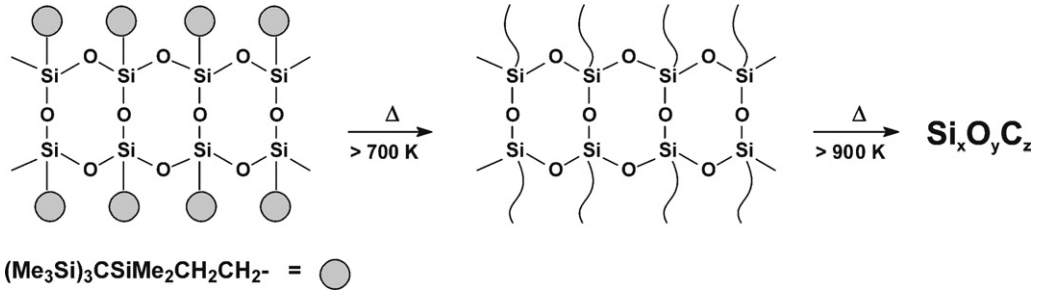

Scheme 2. Ceramization of [tris(trimethylsilyl)methyl]dimethylsilyl-silsesquioxanes at high temperatures.

Scanning electron microscopy was performed using SEM scanning electron microscope JSM-5500 LV (Jeol) apparatus with samples attached to brass supports using an adhesive tape, and their surface was sputter-coated with gold.

Optical images of the films were taken using a digital CCD camera on a Nikon Eclipses E400 POL microscope.

3. Results and discussion

Due to the specific structure of $PT_{Si}SS$, having mixed carbosilane and silsesquioxane characteristics, thermolysis of $PT_{Si}SS$, should be examined taking into account the distinct character of these constituents. Pyrolysis of carbosilane materials as silicon carbide precursors has been well studied [11]. For example, Corriu and co-workers have shown that the thermal degradation of poly(dimethylsilylethylene) (PDMSE) under argon atmosphere proceeds by a random chain scission via a simple free-radical mechanism at 700–800 K [44]. The rate of thermolysis of covalent bonds into radicals is governed by their dissociation energy [45]. Considering a significant length difference between inner Si—C and lateral Si—CH_3 bonds in T_{Si} moiety, [40,41] a preferential degradation of the former might be expected. Besides Si—C bonds fission also redistribution of Si—O and Si—C bonds can be anticipated during the ceramization of $PT_{Si}SS$. The decomposition pathways of $PT_{Si}SS$ were thus compared to these observed for a ladder-like polymethylsilsesquioxane, and studied by TGA/DTA, TG-MS and FTIR techniques, both in inert and oxidative atmosphere.

3.1. Thermogravimetric analysis of $[(Me_3Si)_3CSiMe_2CH_2CH_2SiO_{3/2}]_n$ and $(MeSiO_{3/2})_n$

The thermal characteristics of the studied materials proved their different stabilities. $PT_{Si}SS$ were found to be thermally stable (5% weight loss was detected only at about 700 K under N_2) and a substantial char residue (~24% for $PT_{Si}SS$-I and 33% $PT_{Si}SS$-II) was left at 1200 K in N_2. The results obtained in N_2 (Fig. 1) indicate that the one stage decomposition of both $PT_{Si}SS$-I and $PT_{Si}SS$-II occurs sharply with an onset at 670 K and a steady rate between 680 and 800 K. The maximum velocity of weight decrease corresponds to the temperature of Si—C bonds scission (~720 K) [44]. PMSS is less thermally stable than $PT_{Si}SS$. Its decomposition starts at temperatures lower of 100 K than it was observed for $PT_{Si}SS$. The multiple step weight loss of PMSS corresponds to the literature data (condensation of residual silanol groups and evolution of H_2 and CH_4) [18,23,26].

Experiments carried out in air (Fig. 2) showed that a sample of PMSS lost its initial weight in two steps, with the respective weight

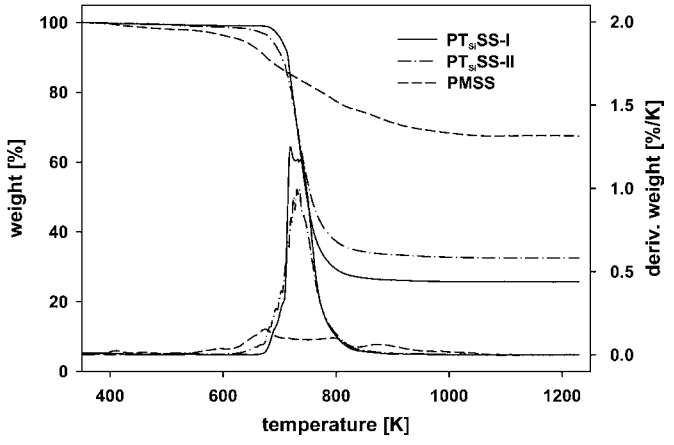

Fig. 1. Thermal decomposition of $PT_{Si}SS$-I, $PT_{Si}SS$-II and PMSS in N_2 (10 K/min).

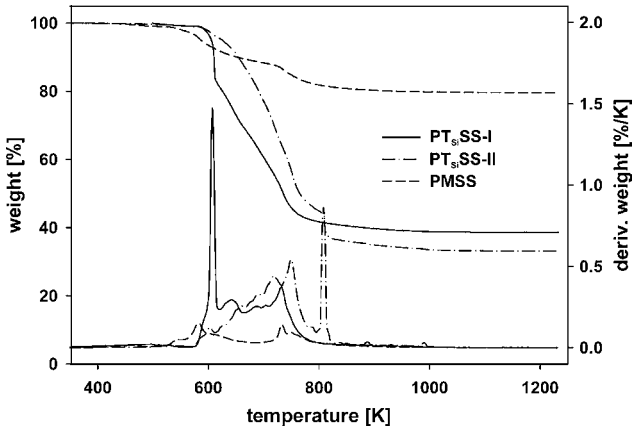

Fig. 2. Thermal decomposition of $PT_{Si}SS$-I, $PT_{Si}SS$-II and PMSS in air (10 K/min).

loss rate maxima at 583 and 733 K. $PT_{Si}SS$ decompose in a different manner and the rate of thermal oxidation varies slightly for crystalline and ladder-like species. The weight reduction of $PT_{Si}SS$-I and PMSS was smaller in air to that in N_2 (chars of 39% and 80% were left, respectively). $PT_{Si}SS$-II left 33% residue at 1200 K. Whereas almost all PMSS was oxidized to silica in air (89.5% residue in theory calculated for conversion of all silicon atoms into SiO_2), for both $PT_{Si}SS$ the residue is too small to prove oxidation of all Si-containing material into silica (calculated 81.2%). A partial degradation on oxidation must have occurred. The formation of volatiles on decomposition of $PT_{Si}SS$ above 570 K in air can be also easily observed using an optical microscope with a heating plate [32]. A thin layer of $PT_{Si}SS$-II was stable up to ~570 K and its melting was not observed. Once the temperature of 570 K was reached, the sample softened and volatile products of its decomposition foamed the material completely over a short time.

3.2. Analysis of gaseous products formed during thermal decomposition

The composition of volatiles formed during the thermal degradation of $PT_{Si}SS$ was studied using a mass spectrometer connected on-line with a TGA apparatus. It enabled simultaneous recording of sample weight decrease and the change of ion current signals during the decomposition. Thermolysis of $PT_{Si}SS$-I, $PT_{Si}SS$-II and PMSS, both in an inert gas atmosphere (helium) and air was carried out and mass spectra were recorded for m/z in the range 10–99. A possible mechanism of thermal degradation of $PT_{Si}SS$ was proposed (Scheme 4). Contrary to our expectations, no increase for ion current corresponding to m/z = 59, 60, 73, 74, which could indicate the species formed due to C—$SiMe_3$ bonds breaking was observed in helium nor air. Instead, ion currents for m/z equal to 15 (CH_3^+), 16 (CH_4^+), 18 (H_2O^+) and 28 ($C_2H_4^+$) were recorded in helium for both $PT_{Si}SS$ and PMSS (Figs. 3a, 4a and 5a). Ion current of m/z = 28 could be also an indicator of CO^+, but since no signal was observed for CO_2^+ (m/z = 44) and the intensity of peak corresponding to $C_2H_3^+$ (m/z = 27) is quite similar to m/z = 28, it seems more appropriate to ascribe m/z = 28 to $C_2H_4^+$, formed by recombination of radicals [46]. TG-MS spectra recorded for $PT_{Si}SS$-I and $PT_{Si}SS$-II are almost identical (Figs. 3a, 4a). The average weight decrease at 1000 K was 68%, which means that a substantial volume of volatiles was formed during the single stage degradation at 700–800 K. Development of CH_3^+ and CH_4^+ was observed within the temperature range of 750–1100 K, but the intensity of the respective ion currents was rather low. It suggests that the major part of volatiles was not detected by the spectrometer (their m/z > 99). The observed sample weight reduction matches the one calcu-

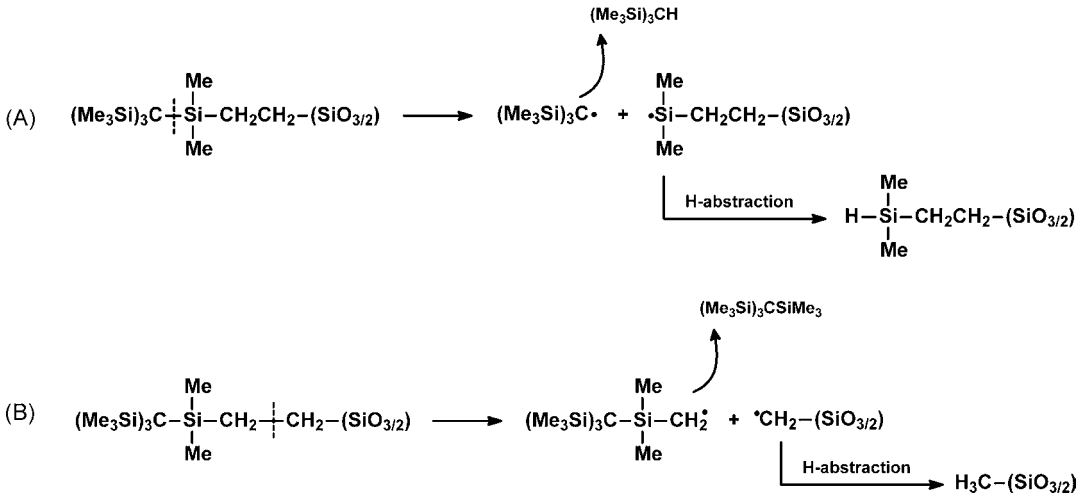

Scheme 4. The proposed free-radical mechanism of decomposition of $PT_{Si}SS$.

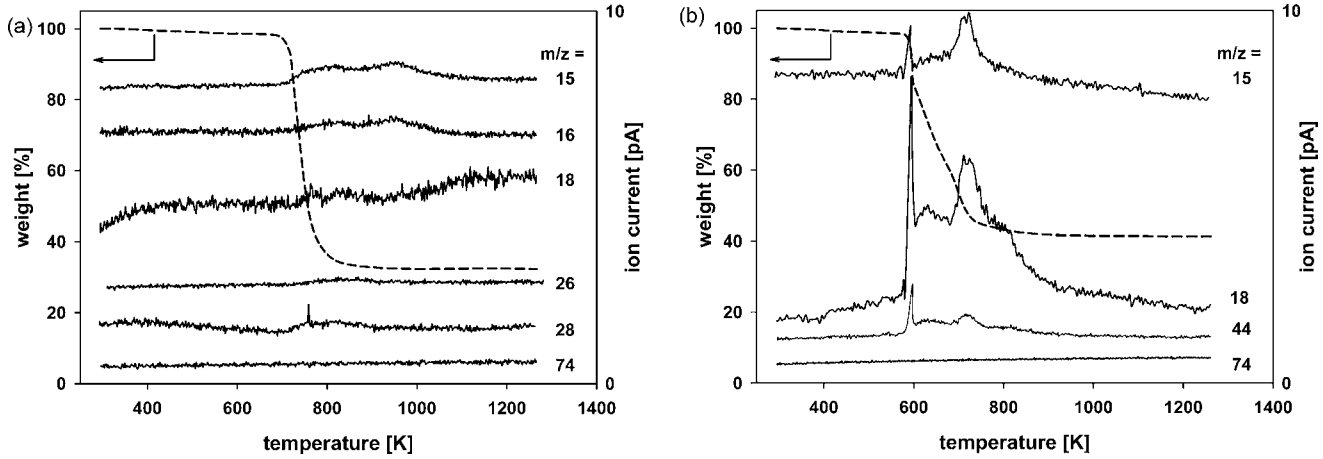

Fig. 3. Thermogravimetric and mass spectrometry results of gaseous products formed during decomposition of $PT_{Si}SS$-I, as a function of thermal curing temperature (a) in helium (10 K/min), (b) in air (10 K/min).

lated for a complete abstraction of $(Me_3Si)_3C$-groups from $PT_{Si}SS$ (Table 1). Such a selective fission of inner Si—C bonds, preceding the cleavage of lateral Si—CH_3 bonds, was observed during pyrolysis of PDMSE [44]. The amount of CH_3^+ and CH_4^+ increases >720 K. It can be explained by condensation of the primary degradation products in upper parts of the heating chamber, and their subsequent decomposition on heating, without the mass decrease in pyrolysed sample. A similar explanation was proposed for evolution of volatiles after a complete thermal degradation of PDMSE [44].

Thermal behaviour of PMSS is typical to a $CH_3SiO_{1.5}$ resin [23,26]. The weight of a sample decreases by 34% after the thermal decom-

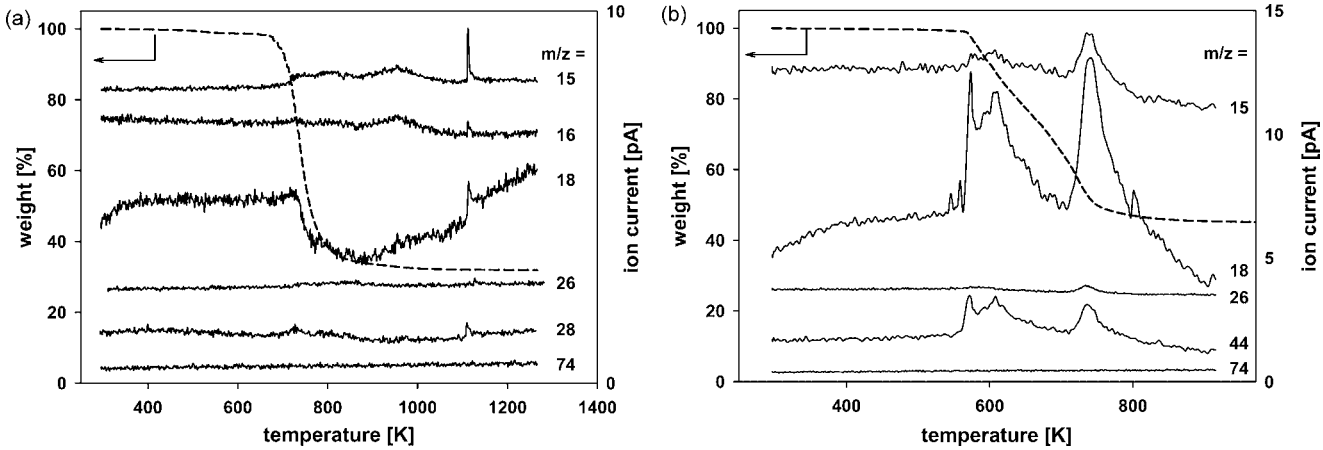

Fig. 4. Thermogravimetric and mass spectrometry results of gaseous products formed during decomposition of $PT_{Si}SS$-II, as a function of thermal curing temperature (a) in helium (10 K/min), (b) in air (10 K/min).

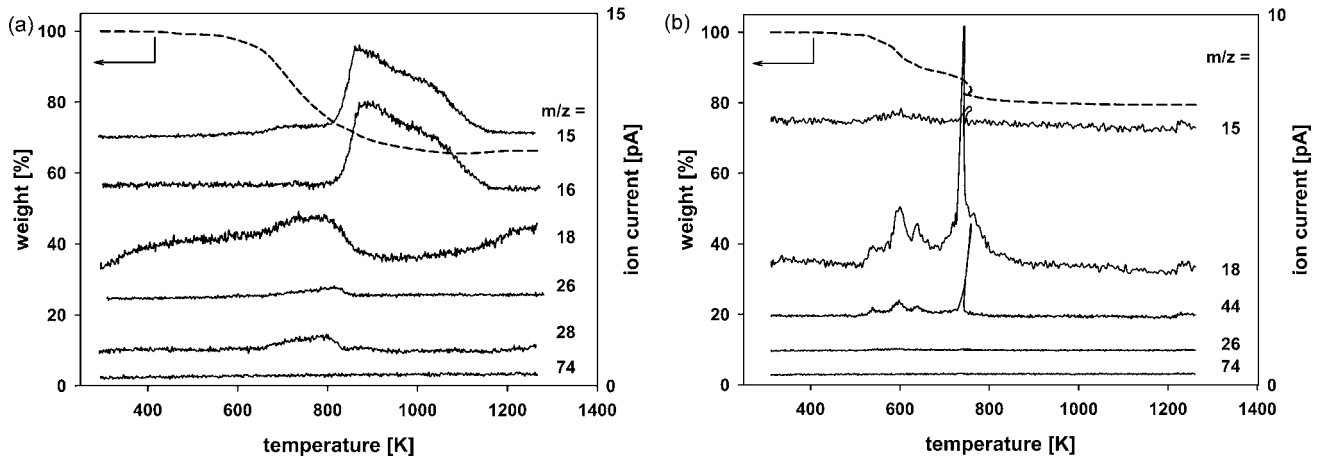

Fig. 5. Thermogravimetric and mass spectrometry results of gaseous products formed during decomposition of PMSS, as a function of thermal curing temperature (a) in helium (10 K/min), (b) in air (10 K/min).

position (Fig. 5a). The first weight loss wave for PMSS, at the temperature range of 600–810 K, corresponds to condensation of the residual silanol groups and H_2O (m/z = 18) removal. At the same temperature signals of m/z = 26, 27, 28 and 29 slightly increase. Ion currents corresponding to products formed by Si—CH_3 bonds rupture [m/z = 15 (CH_3^+) and 16 (CH_4^+)] occur at 800–1100 K. According to the literature data H_2 can be also evolved due to the fission of C—H bonds in this temperature range [26]. The intensity of CH_3^+ and CH_4^+ exceeds these observed for $PT_{Si}SS$, in spite of the relatively smaller amount of Si—CH_3. It supports the postulated decomposition path for $PT_{Si}SS$ with formation of CH_3^+ and CH_4^+ only during a secondary degradation process.

TG-MS analysis of the volatiles released in the oxidative atmosphere (Figs. 3b, 4b and 5b) proved significant differences in the thermal resistance of both types of $PT_{Si}SS$ and PMSS under the applied conditions. The temperature for the main decrease of the sample weight is similar (500–900 K) and the same gaseous species are formed within the temperature range. For all samples CO_2^+ (m/z = 44) and H_2O^+ were the main decomposition products, which points to selective oxidation of Si—C and C—H bonds. In the case of $PT_{Si}SS$ a development of CH_3^+ (m/z = 15) was noted, with maximum of concentration at ~730 K (H_2O^+ and CO_2^+ are still the major components among the detected volatiles). For PMSS a large exothermic effect was observed at this point. The temperature in the heating chamber increased of ~20 K, which caused an automatic switch off of the heating program (initially set for 10 K/min) and some fluctuations in ion currents. The rapid increase in their amount suggests an acceleration of C—H bond oxidation. Such a rapid oxidation of alkyl moieties in silsesquioxane systems was already described by Wang et al. [22]. They reported a simultaneous cleavage and oxidation of alkyl groups in ladder polyepoxysilsesquioxanes, with oxidation intensified once the cleavage was completed. For $PT_{Si}SS$ the intensity of ion currents indicating formation of CH_3^+, CO_2^+ and H_2O^+ seems to depend on the silsesquioxane structure. Their maximum concentrations occur for both $PT_{Si}SS$ at 600–700 and 700–800 K. However, for octahedral $PT_{Si}SS$-I the thermal oxidation begins sharply at 596 K and for ladder-like $PT_{Si}SS$-II it is much less intense. The distinct oxidation rates of $PT_{Si}SS$ and PMSS may be due to the different stability of silsesquioxane and carbosilane systems. The primary oxidation (600–700 K) occurs probably at only a part of methyl groups within $(Me_3Si)_3C$ moiety, whereas the increase in respective ion currents at 700–900 K involves also oxidation of —$SiCH_2CH_2Si$— units.

3.3. FTIR characteristics of structural rearrangements in thermally cured silsesquioxanes

The studied silsesquioxanes show characteristic IR vibrations before the thermal curing (Table 2). After thermolysis of $PT_{Si}SS$ in N_2 and air at 1200 K, IR spectra of both products substantially changed [32]. The Si–O–Si vibrational mode moved towards lower wavelengths. In order to understand the transformations which took

Table 1
Composition of the products of thermal degradation of $[(Me_3Si)_3CSiMe_2CH_2CH_2SiO_{3/2}]_n$.

Sample	Wt%	Calculated[a]		Found	
		C [% wt]	H [% wt]	C [% wt]	H [% wt]
$PT_{Si}SS$-II	–	–	–	41.61	9.93
$PT_{Si}SS$-II[b]	–	–	–	21.03	1.09
$PT_{Si}SS$-II[c]	–	–	–	2.77	0.71
$[(Me_3Si)_3CSiMe_2CH_2CH_2SiO_{3/2}]_n$	100	45.46	10.08	–	–
$[-CSiMe_2CH_2CH_2SiO_{3/2}]_n$	40.6	39.96	6.71	–	–
$[-SiMe_2CH_2CH_2SiO_{3/2}]_n$	37.4	34.74	7.29	–	–
$[-CH_2CH_2SiO_{3/2}]_n$	21.7	29.98	5.03	–	–
$[-CH_2SiO_{3/2}]_n$	17.9	18.17	3.05	–	–
$[-SiO_{3/2}]_n$	14.1	0.00	0.00	–	–
$[MeSiO_{3/2}]_n$	100	17.89	4.51	–	–
$[-SiO_{3/2}]_n$	77.6	0.00	0.00	–	–

Wt%—weight % calculated in respect to the parent silsesquioxane.
[a] Calculated wt% for completely condensed structures.
[b] Heated in N_2 flow.
[c] Heated in air flow.

Table 2
FTIR absorptions for studied silsesquioxanes.

Vibrational assignments	Sample	Frequency of IR band [cm^{-1}]				
		$PT_{Si}SS$-I	$PT_{Si}SS$-II	PMSS	(a)	(b)
ν(C–H) a		2960	2961	2976	–	–
ν(C–H) s		2896	2896	2912	–	–
ν(Si–H)		–	–	–	2100	–
δ(Si–CH_3) a		1408	1408	1410	–	–
δ(Si-CH_3) s		1261	1261	1273	1260	–
ω($SiCH_2CH_2Si$)		1146	1146	–	–	–
ν(Si–O–Si) a		1121	1117	1127	1055–1114	1060-1110
ν(Si–O–Si) s		–	1065	1038	–	–
δ(Si–CH_2-Si)		–	–	–	1055	–
ν(Si–OH)		–	950	960	–	–
δ(Si–O)		–	–	–	784–807	784–807
ρ(Si–CH_3)		855	855	778	–	–
ν(Si–C)		674	674	–	–	–

(a) New IR bands found in samples cured in N_2.
(b) New IR bands found in samples cured in air.
ν—stretching, δ—deformation, ρ—rocking, ω—wagging, a—antisymmetric, s—symmetric.

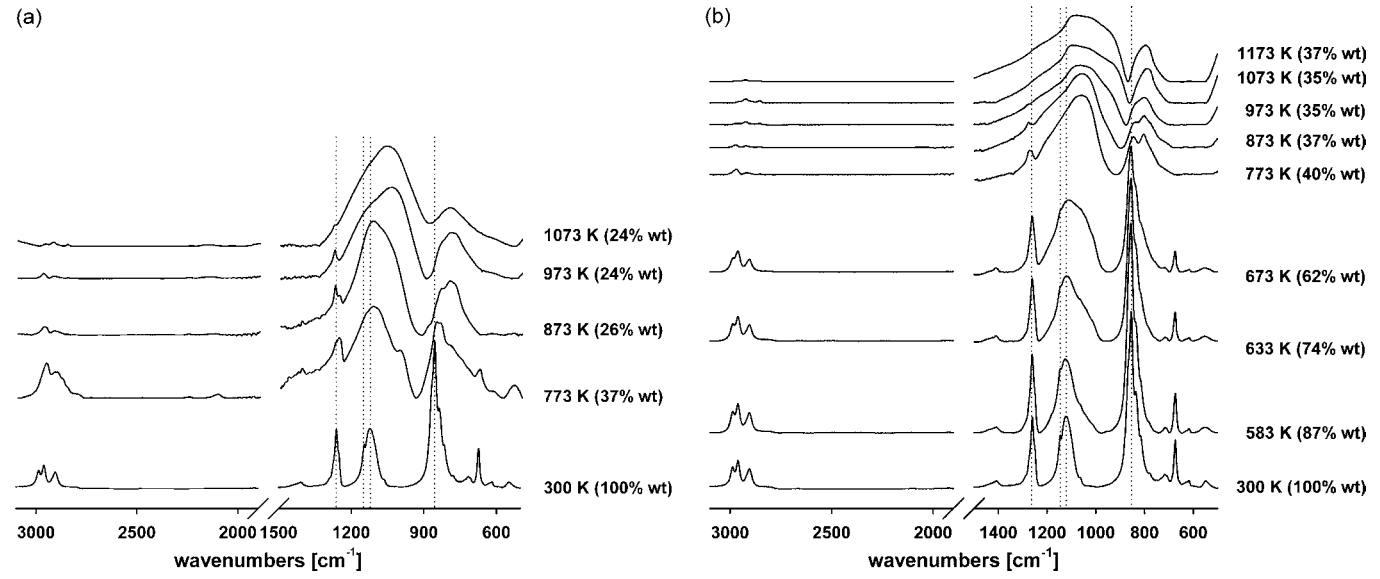

Fig. 6. FTIR spectra of $PT_{Si}SS$-I, as a function of thermal curing temperature (a) in N_2 (20 K/min), (b) in air (20 K/min).

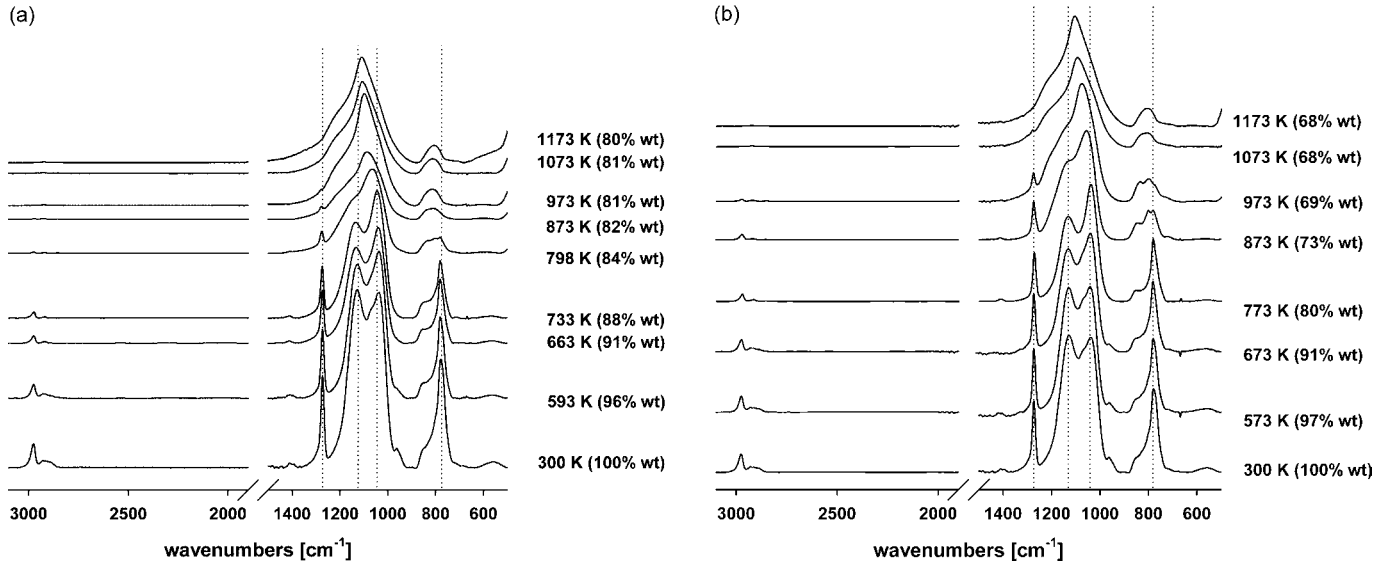

Fig. 7. FTIR spectra of PMSS, as a function of thermal curing temperature (a) in N_2 (20 K/min), (b) in air (20 K/min).

place during the thermolysis of $PT_{Si}SS$ and PMSS, both in inert and oxidative atmosphere, it was necessary to study the structure evolution of the obtained chars. The samples of crystalline $PT_{Si}SS$-I as well as ladder-like $PT_{Si}SS$-II and PMSS were thus heated in N_2 and air to selected temperatures, corresponding to significant changes that were observed during TG-MS analysis. The respective chars were collected and their FTIR spectra were recorded (Figs. 6 and 7 and [32]).

3.3.1. Pyrolysis in an inert atmosphere

Fig. 6a shows changes in FTIR spectra of $PT_{Si}SS$-I as a function of the temperature of curing in N_2. Sample collected at 773 K corresponds to the largest weight decrease [63%, calculated for a total abstraction of $(Me_3Si)_3C$-groups (Table 1)]. Its FTIR spectrum proved a substantial diminishing of the amount of carbosilane substituents [decrease in ν(C–H), ρ(Si–CH_3) and δ(Si–CH_3)]. These results correspond to TG-MS data, and can support the thesis of a rapid abstraction of carbosilane groups at ~720 K. A small amount of Si–H groups was found in the product heated up to ~770 K. The proposed mechanism of thermolysis of $PT_{Si}SS$ (Scheme 4), similar to that proposed for degradation of poly(dimethylsilylethylene) [44], involves the homolytic cleavage of Si–C bonds, followed by hydrogen abstraction from C–H bonds and formation of ≡Si–H. Concomitant transformations can give also ≡Si–CH_2–Si≡ and ≡Si–CH_3 linkages. IR bands corresponding to ≡Si–H and ≡Si–CH_3 were observed at 2100 and 1260 cm^{-1} in the material heated at 773 K (Fig. 6a). Formation of a cross-linked network of a regular arrangement of Si–O–Si bonds was evidenced during the initial stages of thermolysis. Sharp ν(Si–O–Si) band in the octahedral substrate shifted to lower frequencies and became broader. Two new bands appeared as its shoulders at 1055 and 1010 cm^{-1}. The former can be related to ≡Si–CH_2–Si≡ units [47] and the latter to ν(Si–O–Si) in the cross-linked network [30]. At 773–873 K the weight of the sample decreased by another 11%. The majority of Si–O–Si bonds are still arranged in a cage-like network [ν(Si–O–Si) is placed at ~1110 cm^{-1}]. The weight loss at 873–1073 K, corresponding to CH_4 evolution in TG-MS, is insignificant. However, the transformation of siloxane bonds into an extended system with a loss of cage structure is evident. A similar behaviour was noted for $PT_{Si}SS$-II, [32] which also lost most of carbosilane groups at ~720 K and its ladder-like structure gradually turned into a $Si_xO_yC_z$ network. The char obtained from $PT_{Si}SS$ at 773 K was transparent and almost colourless. The increase in the temperature gave the cured samples brown to black colour. It was also noted that the collected chars adhere well to the surface of the platinum pan they were heated in. The strength of adherence decreased with the curing temperature as the chars become more brittle.

Thermal decomposition of PMSS containing four-fold siloxane rings in its structure proceeds differently to those observed for $PT_{Si}SS$ (Fig. 7a). Only 10% sample weight decrease was noted up to ~700 K and any Si–H groups were detected in the FT-IR spectrum of the char obtained at this temperature. Polycondensation of residual silanol groups takes place at 600–770 K, which corresponds to H_2O evolution in TG-MS. ν(Si–O–Si) modes changed on heating, indicating a decrease in structure regularity >800 K. A small amount of Si–C bonds is present even at 973 K. A similar behaviour was reported for other PMSS resins [23,26].

3.3.2. Thermolysis in an oxidative atmosphere

In air $PT_{Si}SS$-I undergoes structural transformations at much lower temperatures than in N_2 (Fig. 6b, [32]). Cross-linking begins at ~580 K, which is indicated by a broadening of ν(Si–O–Si) band. However, $(Me_3Si)_3CSiMe_2CH_2CH_2Si$–groups were not much affected, judging from only a partial decrease of ν(C–H), ρ(Si–CH_3) and δ(Si–CH_3) absorption bands. In spite of oxidation of H–C bonds and rupture of some Si–CH_3 linkages (formation of H_2O^+, CO_2^+ and CH_3^+ indicated by TG-MS), –$SiCH_2CH_2Si$– units remain intact, which is proved by the presence of ω(CH_2) band in the char up to 673 K. Si–H groups are not formed during the thermooxidation. At high temperatures (>900 K), a transformation of organized siloxane structures into a random silica network occurs. The residue obtained at 1073 K in air exceeds the one formed in the inert atmosphere due to oxidation of carbosilane groups into silica. The structural conversion of PMSS at 500–730 K in air (Fig. 7b) proceeds similarly as in N_2 atmosphere. However, the exothermic oxidation recorded by TG-MS at ~740 K induces some differences in the structure of chars. Instead of gradual development of new Si–O–Si bonds, a less regular network is formed >800 K in air.

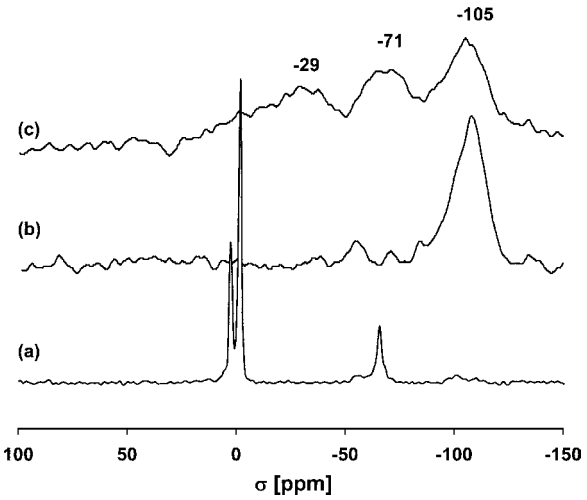

Fig. 8. ^{29}Si MAS NMR spectra of $PT_{Si}SS$-II (a) before and after ceramization (10 K/min) in (b) air and (c) N_2.

3.4. Structural studies (NMR, XRD, SEM) of ceramic products obtained by thermolysis of $PT_{Si}SS$-II

High temperature (1200 K) pyrolysis and thermooxidation were carried out using a sample of $PT_{Si}SS$-II. ^{29}Si and ^{13}C MAS NMR of products (Figs. 8 and 9) indicated structural changes in the studied material and the removal of T_{Si}-group at high temperatures. Resonance lines corresponding to silicon atoms in $(Me_3Si)_3CSiMe_2CH_2CH_2$-groups of $PT_{Si}SS$ substrate (2.7 ppm

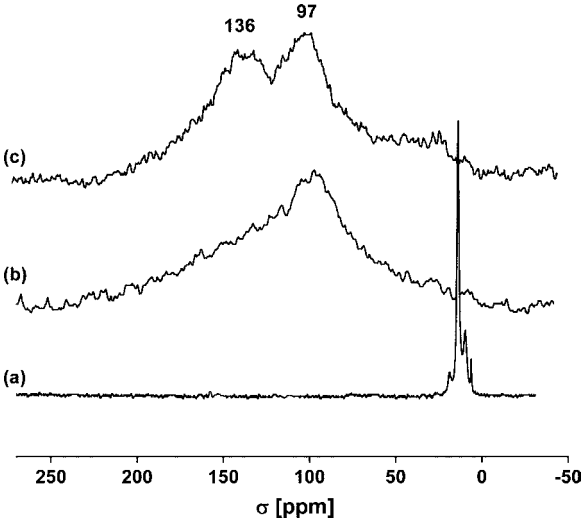

Fig. 9. ^{13}C MAS NMR spectra of $PT_{Si}SS$-II (a) before and after ceramization (10 K/min) in (b) air and (c) N_2.

$SiMe_2$, −1.4 ppm $SiMe_3$) disappeared. MAS NMR spectra of the chars obtained in N_2 and air differ substantially. Broad resonances, that can prove a decrease in order in the material structure and formation of cross-linked $Si_xO_yC_z$ network, appeared in the char obtained in N_2 (Fig. 8). ^{29}Si MAS NMR spectrum of the char shows at least three {−29 ppm D [$(SiO_2)SiC_2$], −71 ppm T_3 [$(SiO)_3SiC$], −105 ppm Q [$(SiO)_4Si$]} of the five possible Si structural units [48–50]. It confirmed that redistribution reactions, involving Si–O and Si–C bonds, took place in N_2 during the polymer-to-ceramic transformation. ^{29}Si MAS NMR of the corresponding sample obtained in air shows one dominating and relatively sharp peak at −105 ppm {along with a minor one ∼−60 ppm [T_2, $(HO)(SiO)_2SiC$]} [51]. It indicates an almost complete Si–C bond scission in air under the studied conditions. The shape of Si–O–Si IR bands in two ceramic products also differed substantially [32]. It confirms the different nature of ceramic network obtained in N_2 and air, shown by ^{29}Si MAS NMR.

^{13}C MAS NMR (Fig. 9) exhibits a broad peak ∼140 ppm, characteristic to free amorphous sp^2 carbon phase [21,27,48,52]. The peaks corresponding to Si–CH_3 groups are no longer present in the aliphatic C range, except a set of broad peaks of low intensity that can be seen in the range 10–30 ppm. They can indicate the products of Si–O and Si–C bonds redistribution at high temperatures [21,27,48,49]. For both samples, cured in N_2 and air, a broad peak shifted upfield to the resonance of free amorphous carbon was present (centred at ∼100 ppm). Resonances of C–O–Si and C=CH linkages in silicon–carbon unsaturated compounds formed during thermolysis of acylpolysilanes [53,54] as well as these of di-O-alkyl groups [55] can be found in this region. Oxidation during pyrolysis in N_2 can be explained by the reaction with trace amount of concomitant oxygen [19,56].

Elemental analysis has proved a substantial decrease in the content of carbon and hydrogen in both chars (Table 1). The carbon load in the char obtained in N_2 is quite significant (50% of the original value) contrary to the hydrogen amount (respectively 11%). Due to the formation of CO_2, the amount of free carbon residue in the char formed in the oxidative atmosphere is much lower (7% of the amount found for the substrate, accompanied by 93% decrease in the hydrogen content). The results confirm the postulated formation of $Si_xO_yC_z$ network in the inert atmosphere, and correspond to the detected free amorphous carbon phase.

$PT_{Si}SS$-II before thermolysis has two broad Bragg halos, which in polymeric silsesquioxanes can be an indicator of a ladder-like organization of siloxane bonds [57,58]. The intramolecular chain-to-chain distance [i.e. the width of each double-chained ladder-like molecule] in $PT_{Si}SS$-II is close to 17.3 Å, whereas the spacing of 7.5 Å corresponds the average thickness of the ladder-like polymer. A preliminary SAXS measurement showed also a lamellar arrangement of 4.1 nm in $PT_{Si}SS$-II. The order in $PT_{Si}SS$-II was completely lost after the thermolysis. The ceramic materials obtained at 1200 K, both in N_2 and air are amorphous [32].

4. Conclusion

Thermal degradation of a new class of hybrid materials, carbosilane–silsesquioxanes ($PT_{Si}SS$) has been studied. $PT_{Si}SS$ are thermally stable up to ∼700 K in N_2 and ∼580 K in air. The studies have shown that contrary to the UV-laser induced photolysis of T_{Si} group, $PT_{Si}SS$ do not decompose at high temperatures by selective degradation of C_q–Si bonds in T_{Si} moiety and loss of Me_3Si-groups. Instead, free-radical abstraction of $(Me_3Si)_3CSiMe_2$- unit from the octahedral or ladder-like silsesquioxane was detected by FTIR, and indirectly confirmed by TG-MS. Above 900 K the transformation of siloxane bonds of $PT_{Si}SS$ into $Si_xO_yC_z$ materials occurs in N_2 and into Si_xO_y in air. Ceramics obtained from $PT_{Si}SS$ (both in air and in N_2) are monolithic materials. The decomposition pathway has an effect for the carbon content in the ceramic product obtained from $[(Me_3Si)_3CSiMe_2CH_2CH_2SiO_{3/2}]_n$. Additionally, evolution of volatiles formed during decomposition of T_{Si} group can increase the porosity of $Si_xO_yC_z$ char.

Acknowledgements

The financial support by Polish Ministry of Science and Higher Education (Grant NR 05-0005-04) is kindly acknowledged. The authors thank Dr. hab. Zbigniew Bartczak [Department of Polymer Physics, CMMS, PAS (SAXS measurement)] and Mgr Sylwia Gmach [Laboratory of Microanalysis, CMMS, PAS (thermolysis and FTIR measurements)] for their kind help. TG-MS analyses were carried out at Faculty of Materials Science and Ceramics, AGH and valuable comments from Prof. Barbara Małecka are kindly acknowledged.

Appendix A. Supplementary data

Supplementary data associated with this article can be found, in the online version, at doi:10.1016/j.tca.2009.04.016.

References

[1] R.H. Baney, M. Itoh, A. Sakakibara, T. Suzuki, Chem. Rev. 95 (1995) 1409–1430.
[2] A. Provatas, J.G. Matisons, Trends Polym. Sci. 5 (1997) 327–332.
[3] J.J. Schwab, J.D. Lichtenhan, Appl. Organometal. Chem. 12 (1998) 707–713.
[4] G. Li, L. Wang, H. Ni, Ch.U. Pittman Jr., J. Inorg. Organomet. Polym. 11 (2001) 123–154.
[5] C. Sanchez, B. Julian, P. Belleville, M. Popall, J. Mater. Chem. 15 (2005) 3559–3592.
[6] K. Pielichowski, J. Njuguna, B. Janowski, J. Pielichowski, Adv.Polym. Sci. 201 (2006) 225–296.
[7] B.J. Chama, B. Kimb, B. Junga, J. Non-Cryst. Solids 352 (2006) 5676–5682.
[8] M.S. Soh, A.U.J. Yap, A. Sellinger, Eur. Polym. J. 43 (2007) 315–327.
[9] Y.R. Liu, Y.D. Huang, L. Liu, Composites Sci. Tech. 67 (2007) 2864–2876.
[10] H. Cao, R. Xu, D. Yu, J. Appl. Polym. Sci. 109 (2008) 3114–3121.
[11] R.J.P. Corriu, Angew. Chem. Int. Ed. 39 (2000) 1376–1398.
[12] R.A. Mantz, P.F. Jones, K.P. Chaffee, J.D. Lichtenhan, J.W. Gilman, Chem. Mater. 8 (1996) 1250–1259.
[13] C. Bolln, A. Tsuchida, H. Frey, R. Mülhaupt, Chem. Mater. 9 (1997) 1475–1479.
[14] A. Fina, D. Tabuani, F. Carniato, A. Frache, E. Boccaleri, G. Gamino, Thermochim. Acta 440 (2006) 36–42.
[15] E.O. Dare, G.A. Olatunji, D.S. Ogunniyi, J. Appl. Polym. Sci. 93 (2004) 907–910.
[16] N. Takamura, L. Viculis, C. Zhang, R.M. Laine, Polym. Int. 56 (2007) 1378–1391.
[17] Y.-C. Sheen, C.-H. Lu, C.-F. Huang, S.-W. Kuo, F.-C. Chang, Polymer 49 (2008) 4017–4024.
[18] V. Belot, R.J.P. Corriu, D. Leclerq, P.H. Mutin, A. Vioux, J. Mater. Sci. Lett. 9 (1990) 1052–1054.
[19] R.M. Laine, J.A. Rahn, K.A. Youngdahl, F. Babonneau, M.L. Hoppe, Z.-F. Zhang, J.F. Harrod, Chem. Mater. 2 (1990) 464–472.
[20] C.T. Chua, G. Sarkar, X. Hu, J. Electrochem. Soc. 145 (1998) 4007–4011.
[21] V. Gualandris, D. Hourlier-Bahloul, F. Babonneau, J. Sol-Gel Sci. Tech. 14 (1999) 39–48.
[22] J. Wang, C. He, Y. Lin, T.S. Chung, Thermochim. Acta 381 (2002) 83–92.
[23] J. Ma, L. Shi, Y. Shi, S. Luo, J. Xu, J. Appl. Polym. Sci. 85 (2002) 1077–1086.
[24] W.-C. Liu, C.-C. Yang, W.-C. Chen, B.-T. Dai, M.-S. Tsai, J. Non-Cryst. Solids 311 (2002) 233–240.
[25] S. Yu, T.K.S. Wong, X. Hu, K. Pita, Chem. Phys. Lett. 380 (2003) 111–116.
[26] G. Trimmel, R. Badheka, F. Babonneau, J. Latournerie, P. Dempsey, D. Bahloul-Houlier, J. Parmentier, G.D. Soraru, J. Sol-Gel Sci. Tech. 26 (2003) 279–283.
[27] B. Toury, F. Babonneau, J. Eur. Ceram. Soc. 25 (2005) 265–270.
[28] A. Gonzalez-Campo, B. Boury, F. Texidor, R. Núñez, Chem. Mater. 18 (2006) 4344–4353.
[29] H. Liu, J. Xu, Y. Li, B. Li, J. Ma, X. Zhang, Macromol. Rapid Commun. 27 (2006) 1603–1607.
[30] V.V. Kireev, B.I. D'yachenko, V.P. Rybalko, Polym. Sci. Series A 50 (2008) 394–402.
[31] A. Kowalewska, W. Fortuniak, B. Handke, J. Organomet. Chem. 694 (2009) 1345–1353.
[32] Supporting Information file.
[33] A. Kowalewska, W.A. Stańczyk, S. Boileau, L. Lestel, J.D. Smith, Polymer 40 (1999) 813–818.
[34] A. Kowalewska, W.A. Stańczyk, Chem. Mater. 15 (2003) 2991–2997.
[35] A. Kowalewska, J. Kupcik, J. Pola, W.A. Stańczyk, Polymer 49 (2008) 857–866.
[36] A. Kowalewska, B. Delczyk, J. Chruściel, e-Polymers (2009), no 013.
[37] K.D. Safa, M. Babazadeh, H. Namazi, M. Mahkam, M.G. Asadi, Eur. Polym. J. 40 (2004) 459–466.
[38] K.D. Safa, M.H. Nasirtabrizi, Eur. Polym. J. 41 (2005) 2310–2319.
[39] C. Eaborn, J.D. Smith, J. Chem. Soc. Dalton Trans. (2001) 1541–1552.

[40] P.T. Brain, M. Mehta, D.W.H. Rankin, H.E. Robertson, C. Eaborn, J.D. Smith, A.D. Webb, J. Chem. Soc. Dalton Trans. (1995) 349–354.
[41] C.A. Morrison, D.W.H. Rankin, H.E. Robertson, C. Eaborn, A. Farook, P.R. Hitchcock, J.D. Smith, J. Chem. Soc. Dalton Trans. (2000) 4312–4322.
[42] A. Kowalewska, K. Rózga-Wijas, M. Handke, e-Polymers (2008), no 150.
[43] M. Handke, A. Kowalewska, W. Mozgawa, J. Mol. Struct. 887 (2008) 152–158.
[44] R.J.P. Corriu, D. Leclerq, P.H. Mutin, J.-M. Planeix, A. Vioux, Organometallics 12 (1993) 454–462.
[45] I. Mita, in: H.H.D. Jellinek (Ed.), Aspects of Degradation and Stabilization of Polymers, Elsevier, New York, 1978 (chapter 6), pp. 247–291.
[46] A.M. Wilson, G. Zank, K. Eguchi, W. Xing, B. Yates, J.R. Darin, Chem. Mater. 9 (1997) 1601–1606.
[47] J. Kurjata, M. Ścibiorek, W. Fortuniak, J. Chojnowski, Organometallics 18 (1999) 1259–1266.
[48] R. Kalfat, F. Babonneau, N. Gharbi, H. Zarrouk, J. Mater. Chem. 6 (1996) 1673–1678.
[49] Q. Liu, W. Shi, F. Babonneau, L.V. Interrante, Chem. Mater. 9 (1997) 2434–2441.
[50] C.G. Pantano, A.K. Singh, H. Zhang, J. Sol-Gel Sci. Tech. 14 (1999) 7–25.
[51] A. Kowalewska, J. Mater. Chem. 15 (2005) 4997–5006.
[52] R.H. Jarman, G.J. Ray, J. Chem. Soc., Chem. Commun. (1985) 1153–1154.
[53] A. Naka, M. Ishikawa, S. Matusi, J. Ohshita, A. Kunai, Organometallics 15 (1996) 5759–5761.
[54] A. Naka, M. Ishikawa, J. Organomet. Chem. 611. (2000) 248–255.
[55] R.V. Law, D.C. Sherrington, Crosslinked Polymers, in: I. Ando, T. Asakura (Eds.), Solid State NMR of Polymers, Elsevier, 1998, p. 534.
[56] K. Matsumoto, H. Matsuoka, J. Polym. Sci. Part A: Polym. Chem. 43 (2005) 3778–3787.
[57] X. Zhang, P. Xie, Z. Shen, J. Jiang, Ch. Zhu, H. Li, T. Zhang, Ch.C. Han, L. Wan, S. Yan, R. Zhang, Angew. Chem. Int. Ed. 45 (2006) 3112–3116.
[58] Z.-X. Zhang, J. Hao, P. Xie, X. Zhang, Ch.C. Han, R. Zhang, Chem. Mater. 20 (2008) 1322–1330.